Integration of Heat Exchanger Models into the Performance Analysis of Innovative Aero Engine Architectures

Marc Schmelcher, Alexander Görtz, Jannik Häßy, Mahmoud El-Soueidan
marc.schmelcher@dlr.de
German Aerospace Center (DLR)
Institute of Propulsion Technology
Cologne
Germany

Fabian Nöske
MTU Aero Engines AG
Engineering Advanced Programs
Munich
Germany

ABSTRACT

Innovative aero engine architectures are needed to tackle the emission reduction goals set. Some of them make use of heat exchangers for heat recovery and thermal management. The Water-Enhanced Turbofan (WET) as one of the innovative and promising concepts incorporates two heat exchangers. An evaporator is one of them and used to preheat, evaporate and superheat liquid water while cooling the turbine exhaust gas. This increases the thermal efficiency of the cycle and increases power density.

The evaporator is one of the key components introduced with the WET concept. Heat exchangers suitable for the WET application were not used in aero engines so far and adequate models have to be developed. From a thermodynamic perspective, the evaporator model needs to predict the transferred heat from the exhaust to the water side and has to account for the pressure losses in both fluids. Additionally, the mass and size of the evaporator are relevant to analyze the options for engine integration and to estimate the overall engine mass.

To the authors' knowledge, there is no method published for an evaporator model used in thermodynamic analysis of aero engines. Therefore, in this paper the following three novel approaches for the thermodynamic analysis of the evaporator introduced in a WET performance model will be investigated and compared: First, the use of a simplified 1D surrogate model in the WET performance model. Second, the iterative integration of a preliminary design tool for heat exchangers into a WET performance model, and third, the direct integration of the same tool into the performance simulation.

The comparison will present differences between computational speed, robustness and accuracy of the approaches. Furthermore, the advantages and disadvantages regarding the different modelling options are discussed and shown exemplarily in a design and an off-design study. In the future, more comprehensive studies of the WET concept are enabled by the use of the presented methods.

Keywords: Water-Enhanced Turbofan (WET); Evaporator; Heat Exchanger; Surrogate Model; Zooming; Coupling; PreHEAT; DLRp2

NOMENCLATURE

CFD	Computational Fluid Dynamics
DLR	German Aerospace Center
DLRp2	DLR performance program (in-house program)
EB	Energy Balance
GTlab	Gas Turbine Laboratory (in-house program)
HRSG	Heat Recovery Steam Generator
MTO	Maximum Takeoff
PLC	Pressure loss coefficient
PreHEAT	Predesign of Heat Exchangers in Aviation (in-house program)
TIT / T4	Turbine inlet temperature or combustor outlet temperature
TSFC	Thrust-specific fuel consumption
WAR	Water-to-Air Ratio
WET	Water-Enhanced Turbofan

Symbols

A	Heat transfer area
htc	Heat transfer coefficient
i	Iterative step
$\dot{m}$	Mass flow
p	Pressure
Δp	Pressure loss
$\dot{Q}$	Transferred heat / heat flow
T	Temperature
ΔT_{min}	Minimum temperature difference
U	Overall heat transfer coefficient

1.0 INTRODUCTION

The Water-Enhanced Turbofan (WET) is one of the currently investigated concepts to tackle the emission reduction goals set to reduce climate impact of aviation. It has the potential to reduce CO2 emissions, NOx emission and condensation trails [1]. Various fields of research have to be combined to assess the feasibility of the concept incorporating new heat exchangers to the aero engine architecture.

One aspect is the overall cycle analysis of the engine concept. In [1] and [2], the authors give an overview over the new components of the WET cycle and present studies considering various water-to-air ratios (WAR), overall pressure ratios and turbine inlet temperatures. The work presented by Kaiser et al. [3] demonstrates the potential of the Water-Enhanced Turbofan to reduce the climate impact of aviation. Görtz et al. [4] discuss the differences, advantages and disadvantages of a hydrogen fueled WET concept compared to a kerosene fueled version of it.

Another research field is the component-based analysis of the WET concept, mainly for the new WET specific components like the condenser, evaporator (also referred to as Heat Recover Steam Generator – HRSG) or the steam injector. Schmitz et al. [5] presented an experimental roadmap for the analyses of the different components within the next years. At the Institute of Propulsion Technology of the German Aerospace Center (DLR) the research focusses on the evaporator of the Water-Enhanced Turbofan. Different fidelity levels are considered, starting on cycle level [4], going to a preliminary design of the evaporator [6] and finally using CFD tools for more detailed analyses of heat exchanger geometries [7]. Experiments will be used to validate and improve the results.

From a thermodynamic perspective, the evaporator model in an engine cycle model needs to predict the transferred heat from the exhaust to the water side and has to account for the pressure losses in both fluids. Going a step further, the mass and size of the evaporator are relevant to analyze the options for engine integration and to estimate the overall engine mass. This directly impacts the fuel burn of the aircraft and has to be considered.

To the authors' knowledge there does not exist a published evaporator model for the incorporation into an aircraft engine performance code.

Therefore, this work is focused on the integration of heat exchanger models into the performance code DLRp2 developed at DLR [8]. Three different options for the evaluation of the evaporator performance in the WET concept are compared in this publication. The first option makes use of a simplified 1D-model of the heat exchanger integrated into the performance code while both other options make use of a coupling between PreHEAT [6], an inhouse tool for *Predesign of Heat Exchangers in Aviation*, and the performance code DLRp2. The coupling allows for a multi-fidelity analysis of the WET concept. All options will be compared regarding computational time, stability, accuracy and the range of capabilities.

After presenting the used tools and coupling methods in chapter 2.0, the three methods for the evaluation of the evaporator performance are described in chapter 3.0. The following chapter 4.0 will present the results of a design variation of the evaporator and its impact on the engine design performance. The accuracy, stability and computational time for the two coupling methods will be analyzed for this study. In chapter 5.0 the off-design results are compared for all three evaporator models in the engine performance. Again, accuracy, stability and computational time will be compared. In the conclusion the three approaches are finally balanced against each other and the best approach is highlighted dependent on the task.

2.0 STATE OF THE ART

GTlab is developed at the DLR Institute of Propulsion Technology as virtual engine framework, where different modules with various fidelity levels can be combined. Therefore, a central data model is used [9]. For this paper, the relevant modules of GTlab are DLRp2 and PreHEAT. They are described briefly in this section.

DLRp2 (*DLR performance program*) is a gas turbine performance code developed at DLR, where various engine components, like intakes, compressors, combustors, turbines, nozzles, etc., can be modelled [8]. Recently, the WET specific components have been added [4]. With those components a WET concept model according to Figure 1 is specified, where the flow path starting from the condenser considering stations 61, 62, 63, 64 and going into the steam injector represents the water loop. The evaporator has two inlets, with station 51 for the turbine exhaust air and station 62 for the liquid, pressurized water. The two outlets are defined by station 6 for the exhaust side and station 63 for the water side. In DLRp2 Design and Off-Design Calculators are used to specify and solve an equation system with certain boundary conditions (e.g. flight conditions) and dependent as well as independent variables. Each component of the engine has its own implemented model to calculate the outlet states based on the inlet states and model parameters. The result of the performance calculation depends on each individual component model. Therefore, it is crucial to implement models that predict the component level performance accurately. In chapter 3.0 the three analyzed options for the evaporator model are presented in detail.

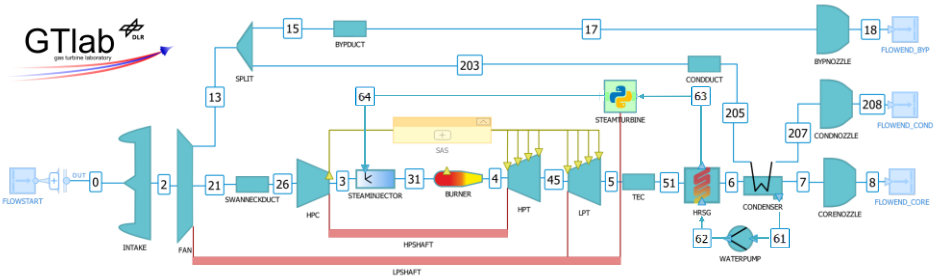

Figure 1 WET performance model representation

PreHEAT (*Predesign of Heat Exchangers in Aviation*) is a preliminary design tool for heat exchangers considering possible phase change developed at DLR. The tool uses the cell-based P-NTU method and correlations for heat transfer coefficient (htc) and pressure loss coefficient on both sides of the heat exchanger to predict the overall heat transfer capability and pressure losses. More details are provided in [6]. The evaporator in the WET concept is a tube bundle heat exchanger with multiple parallel tubes of small diameter. There are several design choices, like the tube diameter, the spacing between tubes, the utilization of fins, the tube length as well as the overall 3D geometry and flow arrangement. A good assessment of the heat exchanger design is only possible, if the engine design and the implications on the overall aircraft design are taken into account.

Using GTlab as a platform, the tools DLRp2 and PreHEAT can be coupled to generate a multi-fidelity simulation, also referred to as *Zooming*. By this means, the geometry and actual performance of the evaporator can be considered during the design and off-design performance analysis of the overall engine. Klein et al. [10] already presented a similar approach using GTlab for the coupling of DLRp2 and the DLR in-house CFD solver TRACE to scale the fan maps of a turbofan engine. Component maps can be derived also for heat exchangers, as presented by Gonser [11] in his dissertation. He uses those heat exchanger maps to model recuperative aero engines. But those heat exchangers are only operated in single-phase and no phase-change takes place. For evaporators with single-phase and two-phase regions, the actual geometry and all inflow conditions significantly influence the heat transfer capability and pressure losses. Therefore, the performance cannot be adequately represented by a low dimensional map. That is why the coupling procedure has to be considered for each individual operating point and automated, fast and stable coupling solutions have to be found. This is called the *Fully Integrated Approach* according to Pachidis [12]. To enable this automated and stable coupling the *direct* coupling approach according to Bolemant [13] is chosen. This is possible since both, DLRp2 and PreHEAT, are provided as Dynamic Link Library (DLL) and coupled directly using GTlab and its data model as mediator.

3.0 METHODS FOR THE EVALUATION OF THE EVAPORATOR PERFORMANCE

The evaporator model in DLRp2 has to calculate the outlet states ($''$) of the evaporator based on the inlet states ($'$) and the expected thermodynamic behavior of the heat exchanger. According to mass conservation law the inlet and outlet mass flow for each side are equal. The outlet pressure can be calculated as the inlet pressure minus the pressure loss for each side. The outlet temperatures can be calculated based on an energy balance for each side using the inlet states and a heat flow, which is equal for both sides. A representation of the model is shown in Figure 2, where the unknown parameters $\dot{Q}, \Delta p_1$ and Δp_2 are highlighted. Those unknown values are needed to calculate the outlet states. Three different approaches to gather those values are presented in this section. The first option is a 1D *Surrogate Model* which is directly incorporated into the DLRp2 performance code. Both other options consider a coupling of DLRp2 and PreHEAT. *Iterative coupling* is used as one option and the other option is a *direct coupling* approach.

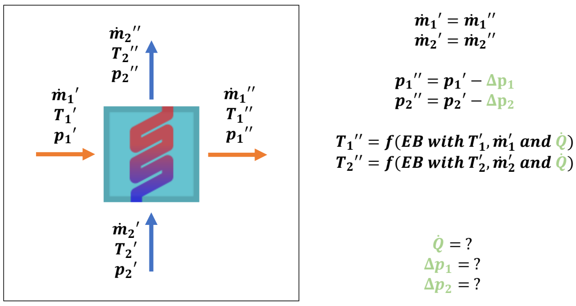

Figure 2 Evaporator model representation

3.1 Surrogate Model of the Evaporator

Using the surrogate model integrated in DLRp2, the transferred heat and pressure losses of the evaporator have to be given for the design calculation by the user as boundary condition. Those boundary conditions are independent of any heat exchanger geometry and can be estimated by the engineer's experience or used as model assumptions that have to be met by an evaporator designer afterwards.

To be independent of absolute values, the pressure losses for both sides are given via a pressure loss coefficient (PLC) according to Equation 1. The transferred heat is also not given as absolute value but the user can specify a minimum temperature difference ΔT_{min} that has to be achieved by the heat exchanger assuming a counterflow evaporator. A temperature profile is calculated using the gas models and an energy balance for both sides. ΔT_{min} can be reached either at the inlet of one of the streams or at the point, where the water enters the two-phase evaporation region. In order to meet the boundary condition, the heat flow is adapted internally until the smallest temperature difference reaches the user specification. The concept of ΔT_{min} as design parameter is further described in [4].

$$PLC_i = \frac{p_i' - \Delta p_i}{p_i{}'} \qquad (1)$$

Based on the given boundary conditions the outlet states of the evaporator fluids can be calculated according to Figure 2. Additionally, the surrogate model analyzes the evaporator using the P-NTU method.

The surrogate model makes use of the cell-based P-NTU method which is also implemented in PreHEAT [6,14]. Unlike in PreHEAT, in the DLRp2 surrogate model major simplifications and assumptions are made. A pure counterflow heat exchanger is assumed with three cells that are sized according to the following sections starting at the water inlet:

1. Liquid Water (preheating)
2. Two-Phase (evaporation)
3. Steam (superheating)

The P-NTU method is applied for each of those cells using the temperature profile calculated by the energy balance. As a result, the product of overall heat transfer coefficient U and heat transfer area A for each cell is calculated. The sum of all cells can be calculated according to Equation 2:

$$UA_{Design} = UA_{1,design} + UA_{2,design} + UA_{3,design} \qquad (2)$$

This value is stored and scaled according to equation 3 for all off-design calculations:

$$UA_{Off-design} = UA_{Design} \cdot \sqrt{\frac{\dot{m}_{exhaust,off-design}}{\dot{m}_{exhaust,design}}} \qquad (3)$$

Equation 3 is derived in [14] based on the justified assumption that the overall heat transfer coefficient of the evaporator is mainly driven by the exhaust side heat transfer coefficient. The water side heat transfer coefficient and wall conduction are orders in magnitude larger than the exhaust side htc and are therefore neglected. The equation results from the simplification of basic correlations for the heat transfer coefficient on the outer side of a tube-bundle heat exchanger.

Using the $UA_{Off-design}$ value for off-design calculations, the transferred heat can be calculated backwards with the P-NTU method for each section and converging the system to a transferred heat $\dot{Q}$, that matches the product of heat transfer area A and overall heat transfer coefficient U according to Equation 2 but for off-design values.

The pressure losses on both sides are calculated during off-design using scalers for the given design pressure losses. Those scalers are calculated based on simplified correlations for pressure losses in tubes and tube-bundles taken from the VDI heat atlas [15]. Additionally, the model needs the estimated tube length, tube diameter, tube roughness and the number of parallel tubes to scale the pressure loss inside the tube. Those values have to be given by engineer's experience again or can be assumed to be boundary conditions for the evaporator designer. More information on the surrogate model implemented in DLRp2 can be found in the thesis of Nöske [14].

The developed surrogate model is intended to be fast and stable. This was tested during extensive performance tests with various flow conditions. Nevertheless, in direct comparison to PreHEAT deviations were identified for the predicted values of $\dot{Q}, \Delta p_1$ and Δp_2. The largest deviations where generally identified for the pressure losses on the water side, inside the tube. This is mainly due to the low discretization of the cell-based P-NTU method and the simplifications regarding the correlations [14]. Furthermore, the surrogate model needs some inputs by the engineer which rely on the experience or assumptions. They can also be given by the results of a higher fidelity tool like PreHEAT for the evaporator. But in this case, there is already a first coupling step integrated for the design calculation.

3.2 Iterative Coupling of PreHEAT

For iterative coupling, also called external coupling [13], PreHEAT and DLRp2 are called alternating by GTlab. The same performance model as represented in Figure 1 is used but the evaporator calculation routine is substituted using a python script. Instead of using the inbuilt surrogate model of DLRp2, the equations in Figure 2 are solved using inputs for $\dot{Q}, \Delta p_1$ and Δp_2 from PreHEAT.

Those inputs are given for design as well as for off-design calculations, since a fully integrated approach (see section 2.0) is chosen. No surrogate model or map is used. Therefore, the design and the off-design coupling method are identical.

The coupling routine that is implemented in GTlab solves the DLRp2 performance model of the WET concept first, using initial guesses for the pressure losses and the heat transfer in the evaporator. Afterwards, PreHEAT is called directly from GTlab using the results of the last performance calculation and taking the inlet values from stations 51 and 62. If PreHEAT finishes successfully, the resulting new pressure losses and the heat flow are fed back to the DLRp2 solver as input for the evaporator. Those values are kept constant for one DLRp2 calculation. If PreHEAT does not converge, the settings of the PreHEAT solver are modified to improve convergence stability and a new calculation is started until it finishes successfully. If this is not possible the coupling procedure stops.

The iterative routine is monitored and stopped using two criteria. It finishes successfully, when the convergence criteria presented in equations 4 to 6 fall below a defined tolerance. Therefore, the new PreHEAT value is compared with the DLRp2 value of the last iterative step.

$$crit_{1,i} = \frac{\dot{Q}_{PreHEAT,i} - \dot{Q}_{DLRp2,i-1}}{\dot{Q}_{DLRp2,i-1}} \quad (4)$$

$$crit_{2,i} = \frac{PLC_{1_{PreHEAT,i}} - PLC_{1_{DLRp2,i-1}}}{PLC_{1_{DLRp2,i-1}}} \quad (5)$$

$$crit_{3,i} = \frac{PLC_{2_{PreHEAT,i}} - PLC_{2_{DLRp2,i-1}}}{PLC_{2_{DLRp2,i-1}}} \quad (6)$$

It stops unsuccessfully, if the criteria are not below the tolerance after a maximum number of iterations. This can happen, if the models diverge or start to oscillate. Oscillation can occur if the convergence tolerance given for PreHEAT is higher than the tolerance specified for the coupling process.

All PreHEAT calculations are based on a specified geometry that has to be generated before the coupling procedure. By this means, design studies can be conducted, where the influence of a changed evaporator geometry on the engine performance can be evaluated. Additionally, the use of PreHEAT allows to vary the used correlations and assumptions, which influence the calculated evaporator performance. This enables a more sophisticated analysis of the evaporator performance than using the surrogate model presented in section 3.1. But, the use of PreHEAT significantly increases the computational costs to calculate one operating point compared to the surrogate model.

3.3 Direct Coupling of PreHEAT

When PreHEAT and DLRp2 are directly coupled, also referred to as internal coupling in [13], PreHEAT is called directly from the DLRp2 solver. GTlab as a framework only starts the DLRp2 solver and provides the tools to call all operations. Similar to the iterative coupling approach, the evaporator in the performance model is substituted by a python script. For direct coupling, PreHEAT is started from this script and calculates the transferred heat and pressure losses to evaluate the outlet states. This is done in each evaluation step of the DLRp2 solver.

If PreHEAT does not converge, the values from the last converged solution are taken to enable a fast solving routine. Since the DLRp2 solver is gradient based, it analyzes the influence of the independent variables on the dependencies. Therefore, gradients based on small steps are calculated during the convergence process. To improve the overall performance, the PreHEAT solver takes the result from the last calculation as initial values. This improves the computational costs when consecutive PreHEAT calls have very similar or identical inlet values.

In comparison to the iterative coupling, no convergence criteria are required since the evaporator model is directly integrated into the performance model. However, since the gradient-based DLRp2 solver is very sensitive for inconsistencies in the models of the performance components, a special treatment is needed for the incorporated PreHEAT calculation. PreHEAT is solved iteratively and various iteration levels exist inside the code. Therefore, the user is able to define tolerances for each level that must be respected by the solver of PreHEAT. When PreHEAT is called during the calculation of the gradients inside the DLRp2 solver, it might happen that the variation of an independent variable influences the inlet conditions of the evaporator only to such an extent, that the resulting influence on the evaporator performance is below the tolerance of PreHEAT. In this case misleading gradients could be the result. Therefore, after each PreHEAT execution, a check is made to see whether the difference to the result values of the last calculation is below the current PreHEAT tolerance. If this is the case, the results from the last iteration and not the new values are used. In this way, the gradient is identified as zero which yields to better convergence behavior than using false gradients, which could even go into the wrong direction.

In general, the direct coupling has the same advantages and disadvantages compared to the surrogate model like the iterative coupling approach (see chapter 3.2). But, the iterative coupling approach is expected to have differences to the direct coupling regarding convergence time and stability. This shall be analyzed in the following sections.

4.0 DESIGN STUDY

The evaporator follows after the turbine section and is considered as tube-bundle heat exchanger with tubes wound spirally around the engine axis. In this design study the length of each tube, and consequently the number of windings, varies between 18m and 40m in increments of 1m, while all other geometric parameters remain constant. The position and the variation of the tube length is visually represented in Figure 3 using the minimum and maximum boundary of the study. In the engine representation (left side of Figure 3) the evaporator is the red cylindric component behind the core of the engine. The evaporator consists of multiple parallel, spirally wounded tubes. On the right side of Figure 3, one spiral tube for the design with 18m tube length and one with 40m tube length can be compared. All calculations are based on *Cruise* as the design point of the engine. The study omits the use of the surrogate model as this model fails to account for the geometric variations by itself. Integrating the surrogate model with performance estimations by the authors' would not make sense at this point.

Six coupling scenarios to PreHEAT are evaluated for the same design study, comprising three iterative coupling methods and three direct coupling methods. These scenarios involve adjustments in coupling tolerance and cell resolution of PreHEAT, as detailed in Table 1. The convergence results, presented in Table 2, focus on total and average time, considering only converged outcomes. Relative deviations are calculated in comparison to the *Iter A* scenario, with average deviations across all scenarios below 0.4% and a maximum deviation of 1.1%. Notably, deviations increase with decreasing accuracy of PreHEAT and the coupling procedure.

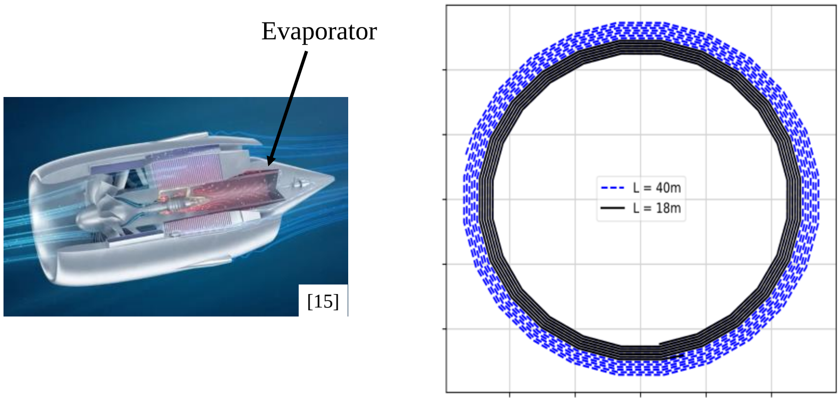

Figure 3 Representation of the tube-bundle evaporator geometry for two different tube lengths (engine footage taken from [16])

Table 1
Coupling scenarios (Design)

	Iter A	**Iter B**	**Iter C**	**Direct A**	**Direct B**	**Direct C**
Coupling type [-]	Iterative	Iterative	Iterative	Direct	Direct	Direct
Coupling tolerance [-]	1e-6	1e-3	1e-3	1e-6	1e-3	1e-3
Geometric resolution [cells/winding]	4	4	1	4	4	1

Table 2
Coupling performance analysis (Design)

	Iter A	**Iter B**	**Iter C**	**Direct A**	**Direct B**	**Direct C**
Total time [sec]	1883.1	595.5	495.3	5035.2	2667.5	1385.7
Average time [sec]	81.9	25.9	21.5	251.8	127.0	63.0
Convergence rate [-]	100 %	100 %	100 %	87 %	91 %	96 %
Average deviation $\dot{Q}$ [-]	0 %	0.007 %	0.308 %	0.045 %	0.040 %	0.259 %
Max. deviation $\dot{Q}$ [-]	0 %	0.016 %	1.010 %	0.452 %	0.086 %	0.968 %
Average deviation PLC_{exh} [-]	0 %	0.001 %	0.022 %	0.002 %	0.010 %	0.012 %
Max. deviation PLC_{exh} [-]	0 %	0.009 %	0.104 %	0.010 %	0.031 %	0.034 %
Average deviation PLC_{wat} [-]	0 %	0.006 %	0.284 %	0.004 %	0.009%	0.234 %
Max. deviation PLC_{wat} [-]	0 %	0.040 %	0.919 %	0.018 %	0.029 %	0.598 %

The study finds that iterative coupling exhibits a superior convergence rate and lower average coupling time compared to direct coupling. For instance, *Iter A* necessitates 6 or 7 iteration steps per design study point, leading to 139 PreHEAT executions for the entire study. Conversely, *Direct A* requires significantly more PreHEAT executions (over 35000), resulting in higher computational costs. Only approx. 20% of those PreHEAT executions are actually relevant, since the other executions led to results with a difference to the previous ones below the tolerance and were therefore neglected (compare chapter 3.3). The deviations of scenarios *A* to *B* are in the same order of magnitude for both, the iterative and the direct coupling method. This is anticipated, as the results should ideally remain independent of the coupling type employed. Iterative coupling proves faster and more stable in total. An adjustment of the coupling tolerance from 1e-06 to 1e-03 demonstrates a 68% reduction in computational costs without significant impact on results. The reduction of the cell resolution does not have a big impact on the convergence time but has higher impact on the result accuracy, even though it is still small. *Iter B* seems to be a good compromise between accuracy and computational costs.

The impact of the design variation on the results of the study is presented in the following, using the *Iter A* results, with all values referenced to a tube length of 30m. The study reveals that transferred heat increases with tube length due to the enlarged heat transfer area but does not follow a linear trend (see Figure 4). This deviation from linearity is attributed to maximum temperature difference limitations between both fluid inlets imposed by engine boundary conditions, causing transferred heat to approach a maximum asymptotically. Selected temperature profiles in Figure 5 show this relationship, where the longer tubes have almost no temperature difference at the water outlet.

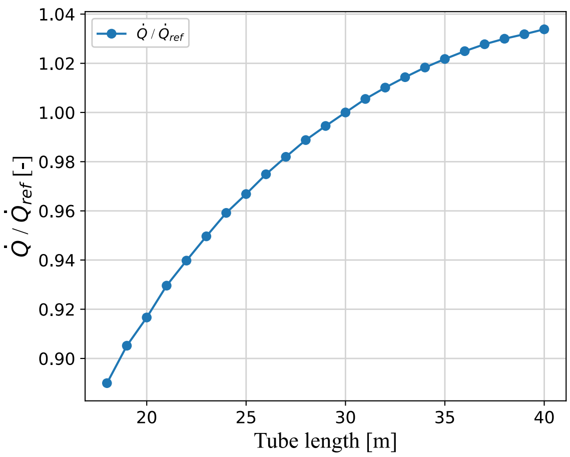

Figure 4 Heat flow in the evaporator as a function of tube length

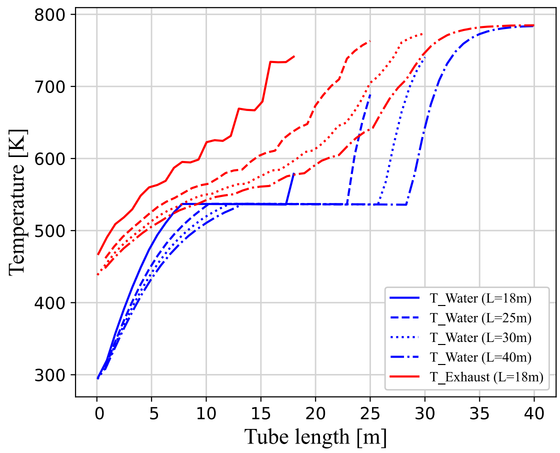

Figure 5 Evaporator temperature profiles for various tube length

Additionally, pressure losses increase with tube length and therefore the PLC decreases (see Figure 6). The exhaust side losses increase due to an increasing number of windings in exhaust flow direction and the water side losses increase due to the longer tube itself, where the water flows through. Oscillations on the water side result from height differences in the heat exchanger and changes in static pressure depending on tube length.

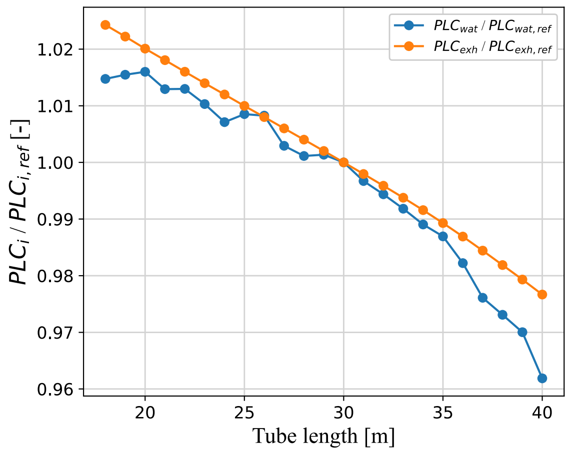

Figure 6 Pressure loss coefficients in the evaporator as a function of tube length

The study identifies a minimum in Thrust Specific Fuel Consumption (TSFC) around a tube length of 35m, as depicted in Figure 7. Notably, the dependency of TSFC on tube length is non-linear, indicating a complex relationship that cannot be depict with a linear surrogate assumption. The design of the evaporator significantly influences TSFC, with variations exceeding 2%.

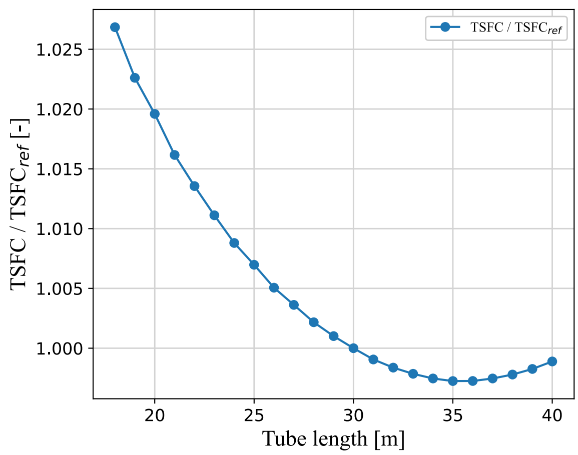

Figure 7 TSFC of the WET concept as a function of tube length of the evaporator

In this analysis, the mass of the heat exchanger increases linearly with tube length. The optimal solution for minimizing fuel burn likely leans towards shorter tube lengths compared to achieving the optimal TSFC. This preference arises from the reduction in weight and size of the heat exchanger, thereby mitigating penalties at the aircraft level. However, a detailed analysis of the fuel burn is out of scope for this publication.

The coupling of the heat exchanger design tool (PreHEAT) with the performance model (DLRp2) enables the exploration of such trade-offs and studies. The results clearly indicate the need for such *Zooming* procedures to identify optimal design solutions. The interaction between engine and heat exchanger performance cannot be represented with simplified assumptions, such as linear extrapolation or constant scaling factors.

5.0 OFF-DESIGN ANALYSIS

The design of the evaporator with a tube length of 30 meters, as presented in Chapter 4.0, has been selected as geometry for this study. In this investigation, the Maximum Takeoff (MTO) operating point is chosen for off-design, providing valuable insights into the performance of the system under varying conditions. The turbine inlet temperature (TIT or T4) in MTO is varied between 1800 K and 2000 K in increments of 10 K to assess the heat exchanger's and engine's behavior across this range. Furthermore, the evaporator models and their influence on the engine are compared to each other.

To have comparable results, the design values for the surrogate model of the evaporator are based on the coupled design analysis in Chapter 4.0. Using this approach, the engines of all three evaporator models result in consistent designs. But, deviations are expected when examining off-design conditions. To explore these variations, five distinct off-design model scenarios are presented, each outlined in Table 3. The scenarios include 2x iterative coupling, 2x direct coupling, and the use of the surrogate model. For the coupled approaches, different tolerances are applied, enabling a nuanced understanding of the system's response to varying levels of precision.

Table 3
Off design evaporator model scenarios

	Iter A	**Iter B**	**Direct A**	**Direct B**	**Surrogate**
Coupling type [-]	Iterative	Iterative	Direct	Direct	None
Coupling tolerance [-]	1e-6	1e-3	1e-6	1e-3	-
Geometric resolution [cells per coil]	4	4	4	4	-

Table 4
Off-design evaporator model performance analysis

	Iter A	**Iter B**	**Direct A**	**Direct B**	**Surrogate**
Total time [sec]	3091.1	1494.9	12978.0	3686.5	493.1
Average time [sec]	147.2	74.7	648.9	245.7	23.5
Convergence rate [-]	100 %	95 %	95 %	71 %	100 %
Average deviation $\dot{Q}$ [-]	0 %	0.006 %	0.005 %	0.043 %	2.742 %
Max. deviation $\dot{Q}$ [-]	0 %	0.016 %	0.007 %	0.078 %	2.874 %
Average deviation PLC_{exh} [-]	0 %	0.001 %	0.001 %	0.002 %	0.765 %
Max. deviation PLC_{exh} [-]	0 %	0.001 %	0.002 %	0.009 %	0.815 %
Average deviation PLC_{wat} [-]	0 %	0.221 %	0.001 %	0.015 %	10.7 %
Max. deviation PLC_{wat} [-]	0 %	0.483 %	0.003 %	0.034 %	13.2 %

The analysis of the coupling scenarios in the current study yielded results comparable to those observed in the initial design study, as illustrated in Table 4, with *Iter A* serving as the reference for comparison. Because of the complexity introduced by more complicated off-design models in all components, not solely attributable to the evaporator model, average computational times were generally longer than those observed during the design calculations. Again, an increased coupling tolerance was found to significantly reduce computational costs, while having a low impact on the precision. Moreover, iterative coupling demonstrated greater stability compared to direct coupling methodologies. However, it was noted that during the iterative coupling process, one off-design point failed to converge, primarily due to unconverged performance models rather than issues inherent to the coupling methodology itself, highlighting the need for robustness-enhancing strategies in future.

Both iterative and direct coupling approaches fell within the prescribed tolerances for the coupling process. Notably, deviations from the surrogate model were found to be greater than those observed between different coupling options, with the most significant deviation observed in water pressure loss, averaging at 10.7%. Despite these variations, the surrogate model demonstrated notable advantages, being more than three times faster than the fastest coupling scenario while successfully converging 100% of the operating points.

The converged results of the off-design study itself are presented in the following, focusing on the scenarios *Iter A* and *Surrogate*, since the results of the other coupling scenarios do not significantly differ from *Iter A*. It is important to note that all values presented have been non-dimensionalized using the values for T4 = 1900 K in the *Iter A* scenario as the reference point.

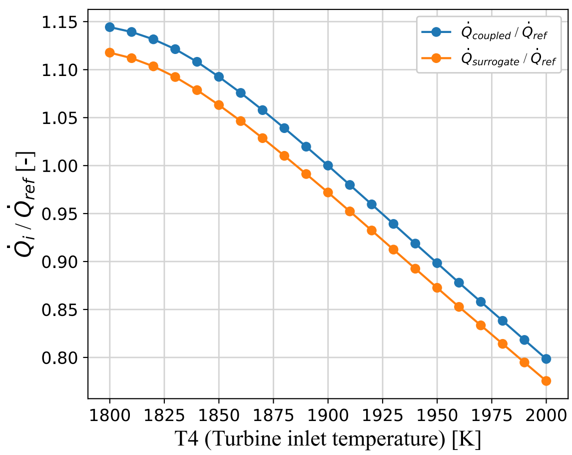

Figure 8 Heat flow in the evaporator as a function of T4 comparing coupled calculation (*Iter A*) and surrogate model

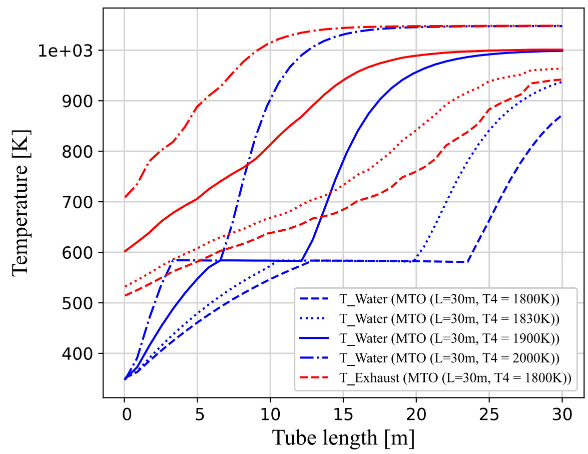

Figure 9 Evaporator temperature profiles for various T4

Analysis reveals that the surrogate model consistently underestimates transferred heat, exhibiting a nearly constant offset of 2.7% across the range of TIT values considered (see Figure 8). Notably, transferred heat decreases as TIT increases. This phenomenon can be attributed to the linear reduction of WAR in the WET concept, which is necessary to elevate temperatures while maintaining constant thrust. Consequently, there is a linear decrease in the maximum transferable heat to the water side and hence, a reduction in heat recovery. However, this linear decrease only holds true when the water reaches the exhaust temperature at the exit of the evaporator, enabling maximum possible heat transfer.

In the low T4 range, a non-linear curve is observed, indicating deviations from the linear trend. This deviation occurs because, at low exhaust temperatures, the evaporator is not capable of superheating the water to the exhaust inlet temperatures, leading to a non-linear dependency. Figure 9 represents the temperature profiles in the evaporator for a few TIT to outline the different water temperatures at the evaporator outlet.

Pressure losses on the water side exhibit the largest deviation between the coupled model and the surrogate model, as presented by Figure 10 and Table 4. This discrepancy arises due to the numerous simplifications implemented in the surrogate model, which aim to reduce complexity but inevitably overlook some of the complex interactions within the evaporator (compare Section 3.1). Anyhow, it is important to note that the influence of water side pressure drop on the overall performance of the engine is relatively minor. This is primarily because variations in water pressure drop can be compensated by adjusting the power of the water pump responsible for supplying liquid water to the evaporator. Furthermore, the power required for liquid water compression is negligible compared to the overall power consumption of the engine. Therefore, inaccuracies in predicting water pressure losses have a limited impact compared to factors such as transferred heat and exhaust side pressure losses.

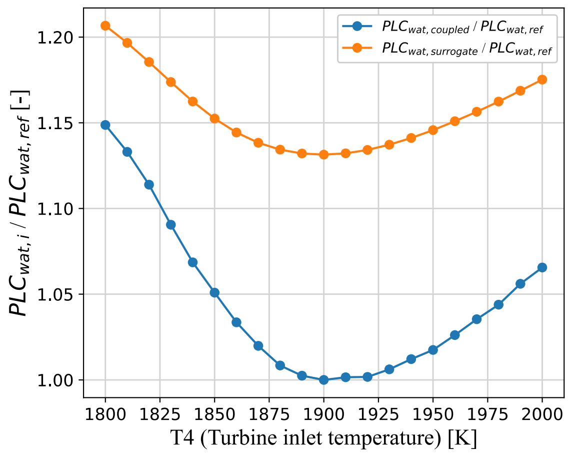

Figure 10 Water side pressure loss coefficient in the evaporator as a function of T4 comparing coupled calculation (*Iter A*) and surrogate model

The surrogate model demonstrates remarkable accuracy in predicting TSFC with deviations of less than 1% compared to the coupled model across all operating points (see Figure 11). An optimum TSFC is identified at the point where transferred heat begins to decrease linearly (as depicted in Figure 8) and the water exits the evaporator with the exhaust gas inlet temperature. From this point on, the recovered heat inside the engine is reduced while the pressure losses on the exhaust side increase with increasing T4. Therefore, the efficiency of the engine is reduced and TSFC increases.

Overall, the surrogate model adequately predicts the off-design characteristics of the evaporator and accurately represents the trends observed in the study. Given the high computational cost associated with coupling, its justification is warranted only for detailed studies. Moreover, it is imperative to ensure appropriate modeling of all components within the WET model to maintain accuracy and reliability in predictive analyses. A high accuracy using a coupled evaporator model cannot compensate for false predictions in other component models.

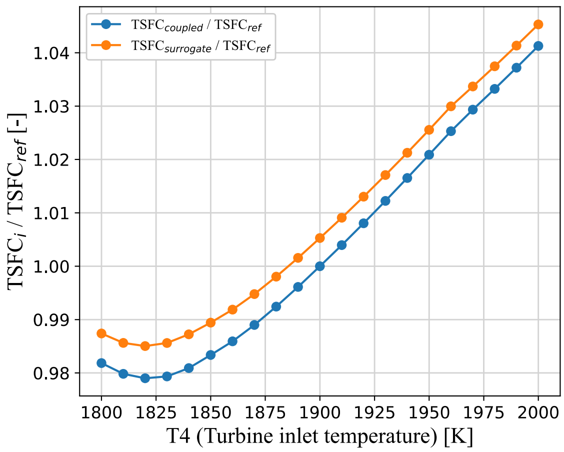

Figure 11 TSFC of the WET concept as a function of T4 comparing coupled calculation (*Iter A*) and surrogate model

6.0 CONCLUSION

In summary, this work presented three different approaches to model the evaporator in the WET concept. One surrogate model and two coupling methods to integrate the results of preliminary heat exchanger design (PreHEAT) into the gas turbine performance analysis (DLRp2). All options where evaluated in a comparative way for both design and off-design analysis of the engine. In addition to the comparison of the approaches, the results of the design and off-design studies itself are presented and discussed.

The coupling of preliminary heat exchanger design (PreHEAT) and gas turbine performance analysis (DLRp2) emerges as a highly relevant approach for design studies of the evaporator in the WET concept, particularly due to its ability to consider all dependencies between evaporator geometry and engine boundary conditions. The iterative/external coupling method has been shown to be both more stable and faster than direct/internal coupling methodologies, with a coupling tolerance criterion of 1e-03 proving to be sufficiently accurate for predictive analyses. Moreover, it has been demonstrated that the discretization of cells within PreHEAT does not significantly impact computational costs but should be sufficiently high to ensure accurate results. Therefore, the iterative coupled solution with a tolerance criterion around 1e-03 will be used in future studies. Approaches to further enhance the robustness of the iterative coupling procedure will be investigated, even if the convergence rate for all iteratively coupled operating points in this work is already above 99%.

Additionally, the surrogate model for off-design studies has shown remarkable efficiency, being more than three times faster than coupling to PreHEAT while maintaining stability and predicting transferred heat and exhaust pressure losses with less than 3% and 1% average deviation, respectively. Although water pressure losses exhibit the largest deviation, exceeding 10% on average, their influence on WET performance is relatively small. Therefore, it is justified to use the surrogate model instead of a coupling procedure for extensive off-design studies and to use only random comparison with a coupled solution. If computational effort allows, the coupling approach can be used instead of the surrogate model for all operating points of a study.

Looking forward, current and future work will focus on further enhancing the fidelity of analyses by coupling PreHEAT to Computational Fluid Dynamics (CFD), enabling multi-fidelity analyses across different levels. Additionally, design studies for the evaporator, including component zooming and variation of geometric parameters within a large design space, will be instrumental in investigating engine performance and optimizing system efficiency.

ACKNOWLEDGMENTS

This research was conducted within the DINA2030+ project funded by the LuFo Aviation Research Program of the German Federal Ministry for Economic Affairs and Climate Action under grant number 20M2110B. Responsibility for the content of this publication lies with the authors. The authors want to thank all project members for the collaboration on the project.

Supported by:

Federal Ministry for Economic Affairs and Climate Action

on the basis of a decision by the German Bundestag

7.0 REFERENCES

[1] O Schmitz et al., “Aero Engine Concepts Beyond 2030: Part 1—The Steam Injecting and Recovering Aero Engine,” *Journal of Engineering for Gas Turbines and Power*, vol. 143, no. 2, 2021.
[2] P Ziegler et al., “PARAMETRIC CYCLE STUDIES OF THE WATER-ENHANCED TURBOFAN CONCEPT,” *Proceedings of the ASME Turbo Expo 2023: Presented at the 2023 ASME Turbo Expo, June 26-30, 2023, Boston, Massachusetts,* Boston, Massachusetts, 6/26/2023 - 6/30/2023, American Society of Mechanical Engineers, New York, NY, 2023.
[3] S Kaiser et al., “The Water-Enhanced Turbofan as Enabler for Climate-Neutral Aviation,” *Applied Sciences*, vol. 12, no. 23, p. 12431, 2022.
[4] A Görtz et al., “WATER ENHANCED TURBOFAN: IMPROVED THERMODYNAMIC CYCLE USING HYDROGEN AS FUEL,” *Proceedings of the ASME Turbo Expo 2023: Presented at the 2023 ASME Turbo Expo, June 26-30, 2023, Boston, Massachusetts,* Boston, Massachusetts, 6/26/2023 - 6/30/2023, American Society of Mechanical Engineers, New York, NY, 2023.
[5] O Schmitz et al., “Aero Engine Concepts Beyond 2030: Part 3—Experimental Demonstration of Technological Feasibility,” *Journal of Engineering for Gas Turbines and Power*, vol. 143, no. 2, 2021.
[6] M Schmelcher et al., “Methods for the Preliminary Design of Heat Exchangers in Aircraft Engines,” *Proceedings of the ASME Turbo Expo 2023: Presented at the 2023 ASME Turbo Expo, June 26-30, 2023, Boston, Massachusetts,* Boston, Massachusetts, 6/26/2023 - 6/30/2023, American Society of Mechanical Engineers, New York, NY, 2023.
[7] M El-Soueidan et al., “Integration of a Gas Model into CFD Analysis for the Simulation of Turbine Exhaust Flows With High Steam Loads,” *Proceedings of the ASME Turbo Expo 2023: Presented at the 2023 ASME Turbo Expo, June 26-30, 2023, Boston, Massachusetts,* Boston, Massachusetts, 6/26/2023 - 6/30/2023, American Society of Mechanical Engineers, New York, NY, 2023.
[8] R-G Becker et al., “DEVELOPMENT OF A GAS TURBINE PERFORMANCE CODE AND ITS APPLICATION TO PRELIMINARY ENGINE DESIGN,” *Deutscher Luft- und Raumfahrtkongress 2011,* Bremen, Germany, 2011.
[9] S Reitenbach et al., “Collaborative Aircraft Engine Preliminary Design using a Virtual Engine Platform, Part A: Architecture and Methodology,” *AIAA Scitech 2020 Forum,* Orlando, FL, American Institute of Aeronautics and Astronautics, Reston, Virginia, 01062020.
[10] C Klein et al., “A Fully Coupled Apporach for the Integration of 3D-CFD Component Simulation in Overall Engine Performance Analysis,” *Proceedings of ASME Turbo Expo 2017: Turbomachinery Technical Conference and Exposition,* Charlotte, NC, USA, June 26-30, 2017.
[11] H Gonser, “Untersuchung zum Einsatz von Wärmetauschern in zivilen Turboflugtriebwerken,” Dissertation, Universität Stuttgart. Institut für Luftfahrtantriebe, Stuttgart 2008.
[12] V Pachidis et al., “A Fully Integrated Approach to Component Zooming Using Computational Fluid Dynamics,” *Proceedings of ASME Turbo Expo 2005: Power for Land, Sea and Air,* Reno-Tahoe, Nevada, USA, June 6-9, 2005.

[13] M BOLEMANT, “Optimierung des stationären Betriebsverhaltens von Zweiwellentriebwerken durch angepasste Leitradverstellung im Hochdruckverdichter,” Dissertation, TU Berlin, Berlin 2023.
[14] Fabian Torsten Nöske, “Modellierung und Bewertung des Off-Design Verhaltens von Verdampfern in der Triebwerksvorauslegung,” Master thesis, TU Berlin. Institut für Luft- und Raumfahrt, Berlin Nov. 2022.
[15] Verein Deutscher Ingenieure, *VDI Heat Atlas*, Springer Berlin Heidelberg, Berlin, Heidelberg, 2010.
[16] MTU AERO ENGINES AG, “Water-Enhanced Turbofan,” https://www.mtu.de/de/technologie/clean-air-engine/water-enhanced-turbofan/ (current as of Feb. 09, 2024).